

## Planar Tetracoordinate Carbon Atoms Centered in Bare Four-membered Rings of Late Transition Metals

Debjeni Roy, Clémence Corminboeuf, Chaitanya S. Wannere, R. Bruce King, and Paul v. R. Schleyer\*

Center for Computational Chemistry and Department of Chemistry, University of Georgia, Athens, Georgia 30602

Received May 10, 2006

Planar tetracoordinate carbons (ptC's) can be stabilized by four-membered ring perimeters composed of four bare transition metal atoms. DFT analyses of the molecular orbitals, electronic structures, energies, and magnetic properties of these  $CM_4$  species (where M represents isoelectronic combinations of Cu, Ni, Ag, and Pd) reveal striking similarities with main group metal ptC analogues (e.g.,  $CAI_2Si_2$ ,  $CAI_4Na^-$ , and  $C_5Li_2$ ). While the  $CCu_4^{2+}$ ,  $CAG_4^{2+}$ , and  $CNiCu_3^+$  ions have the largest HOMO–LUMO separations,  $CCu_4^{2+}$  is the best candidate for detection by gas-phase photoelectron spectroscopy.

## Introduction

Van't Hoff and LeBel's tetrahedral carbon<sup>1,2</sup> pervades chemistry. Planar tetracoordinate carbon (ptC) alternatives were long thought to be too high in energy to be viable<sup>3</sup> until, in 1970, Hoffmann, Alder, and Wilcox formulated "electronic" strategies for reducing the relative energies of ptC structures.<sup>4</sup> The systematic and extensive computational investigation of Schleyer and Pople<sup>5</sup> designed the first example of a ptC molecule, 1,1-dilithiocyclopropane, by employing an additional "mechanical" strategy.<sup>5</sup> The smaller bond angles of the three- and four-membered rings favor ptC's. In addition, the in-plane electron deficiency can benefit from  $\sigma$  donation by electropositive groups. Many compounds with a ptC are now known on the basis of these electronic and mechanical principles.<sup>6–8</sup>

Hoffmann et al.<sup>4</sup> pointed out that the HOMO of planar methane, a p-orbital lone pair on the ptC, could be stabilized by delocalization to  $\pi$  acceptors.<sup>9</sup> In contrast, Wang and Schleyer<sup>10</sup> stressed the conceptual advantages of basing ptC designs on the *inherently planar methane dication* and the stabilization of its vacant ptC p orbital by  $\pi$ -donor substituents. The methane radical cation may be an even better model, since the ptC p orbitals of almost all of the many known examples<sup>11</sup> are occupied by one  $\pi$  electron, more or less. Overall neutrality of the ptC molecules can be achieved by appropriate isoelectronic atom replacements.<sup>10,12a</sup>

Schleyer and Boldyrev (SB) were the first to design ptC's with the minimum number of atoms (five) (e.g., the neutral pentatomic  $CAI_2Si_2$  isomers and their analogues).<sup>12a</sup> The 1991 SB computational predictions were verified experimentally in 1998 by the detection of the isoelectronic anions,  $CAI_3Si$ - $Si$ <sup>12a,12d</sup> and the closely related  $NaCAI_4^-$ .<sup>13</sup> The planarity of such ptC molecules composed of second or third row main group ligand atoms in four-membered ring perimeters is

\* To whom correspondence should be addressed. E-mail: schleyer@chem.uga.edu.

- (1) van't Hoff, J. H. *Arch. Neerl. Sci. Exactes Nat.* **1874**, 445.
- (2) LeBel, J. A. *Bull. Soc. Chim. Fr.* **1874**, 22.
- (3) Monkhorst, H. J. *J. Chem. Soc., Chem. Commun.* **1968**, 1111.
- (4) Hoffmann, R.; Alder, R. W.; Wilcox, C. F. *J. Am. Chem. Soc.* **1970**, *92*, 4992.
- (5) Collins, J. B.; Dill, J. D.; Jemmis, E. D.; Apeloig, Y.; Schleyer, P. v. R.; Seeger, R.; Pople, J. A. *J. Am. Chem. Soc.* **1976**, *98*, 5419.
- (6) For review, sees: (a) Sorger, K.; Schleyer, P. v. R. *THEOCHEM* **1995**, *338*, 317. (b) Rottger, D.; Erker, G. *Angew. Chem., Int. Ed. Engl.* **1997**, *36*, 812. (c) Radom, L.; Rasmussen, D. R. *Pure Appl. Chem.* **1998**, *70*, 1977. (d) Siebert, W.; Gunale, A. *Chem. Soc. Rev.* **1999**, *28*, 367. (e) Minkin, V. I.; Minyaev, R. M.; Hoffmann, R. *Usp. Khim.* **2002**, *71*, 989.
- (7) McGrath, M. P.; Radom, L. *J. Am. Chem. Soc.* **1993**, *115*, 332.
- (8) (a) Rasmussen, D. R.; Radom, L. *Angew. Chem., Int. Ed.* **1999**, *38*, 2876. (b) Rasmussen, D. R.; Radom, L. *Chem.—Eur. J.* **2000**, *6*, 2470.

- (9) Esteves, P. M.; Ferreira, N. B. P.; Correa, R. J. *J. Am. Chem. Soc.* **2005**, *127*, 8680.
- (10) Wang, Z.-X.; Schleyer, P. v. R. *J. Am. Chem. Soc.* **2001**, *123*, 994.
- (11) (a) Lyons, J. E.; Rasmussen, D. R.; McGrath, M. P.; Nobes, R. H.; Radom, L. *Angew. Chem., Int. Ed. Engl.* **1994**, *33*, 1667. (b) Wang, Z.-X.; Schleyer, P. v. R. *J. Am. Chem. Soc.* **2002**, *124*, 11979.
- (12) (a) Schleyer, P. v. R.; Boldyrev, A. I. *J. Chem. Soc., Chem. Commun.* **1991**, 1536. (b) Boldyrev, A. I.; Simons, J. *J. Am. Chem. Soc.* **1998**, *120*, 7967. (c) Li, X.; Wang, L.-S.; Boldyrev, A. I.; Simons, J. *J. Am. Chem. Soc.* **1999**, *121*, 6033. (d) Wang, L.-S.; Boldyrev, A. I.; Li, X.; Simons, J. *J. Am. Chem. Soc.* **2000**, *122*, 7681. (e) Li, X.; Zhai, H.-J.; Wang, L.-S. *Chem. Phys. Lett.* **2002**, *357*, 415.
- (13) Li, X.; Zhang, H.-F.; Wang, L.-S.; Geske, G. D.; Boldyrev, A. I. *Angew. Chem., Int. Ed.* **2000**, *39*, 3630.

characterized by multicenter  $\pi$  bonding involving all of the atoms, as well as peripheral ligand–ligand bonding.<sup>12</sup> Can transition metal rings function effectively as well? Is it possible to have only four transition metal atoms in addition to the ptC?

A square planar carbon inside a four-membered nickel ring moiety has been known for some time in the  $\text{Ca}_4\text{Ni}_3\text{C}_5$  aggregate synthesized by Musanke and Jeitschko.<sup>14</sup> The bonding of the underlying  $\text{CNi}_4$  unit of this unusual nickel carbide polymer network has been analyzed using qualitative, band-structure calculations employing extended Huckel tight-binding theory.<sup>15</sup> The unusual carbide polymer network features infinite, one-dimensional, vertex-sharing chains of Ni squares. Each nickel atom has linear C–Ni–C coordination to the central square planar or external  $\text{C}_2$  with weak  $\text{Ni}\cdots\text{Ni}$  bonding. Inspired by the theoretical study of Tsipis on the hydrocopper  $\text{Cu}_4\text{H}_4$  ring,<sup>16</sup> Li et al. computed a ptC-containing  $D_{4h}$  “hydronickel” compound.<sup>17</sup> We now describe the smallest “naked” transition metal clusters that can host a ptC atom. These predictions developed from our theoretical investigation of bare transition metal rings (i.e., without hydrogen or other substituents).<sup>18</sup> Such rings are inherently well suited to stabilize central atom placements. While we focus on carbon as the central atom here, other elements can function equally well as the central tetracoordinate atom.

### Computational Details

Our design strategy places the ptC inside suitable four-membered late transition metal element rings composed of combinations of Ni and Cu or of their heavier congeners, Pd and Ag. The optimized geometries of these species are rather insensitive to the DFT level. The symmetry-constrained structures reported here are based on the B3LYP functional, together with the standard Karlsruhe valence triple- $\zeta$  valence basis sets augmented with double polarization functions (TZVPP for C, Ni and Cu),<sup>19</sup> or with the LANL2DZ combination of valence and ECP basis sets (Ag, Pd).<sup>20</sup> The Gaussian03 program was employed.<sup>21</sup> The computed vibrational frequencies show the ptC structures in Figure 1 to be minima. The potential energy surfaces were explored using the Saunders “kick” method,<sup>22</sup> newly implemented as an automated procedure.<sup>23</sup> This stochastic method generates structures randomly and facilitates the thorough exploration of unknown isomers much more easily than manual methods. It does not involve any preconceived structures based on bonding principles. Instead, all the atoms are placed at the same point initially and then are “kicked” randomly within a box of chosen dimensions. The kick size was varied from 2.0 to 2.5 Å in the cubic boxes employed here. These initial geometries (in, for example, independent sets of 50 or 100 kick jobs) are then

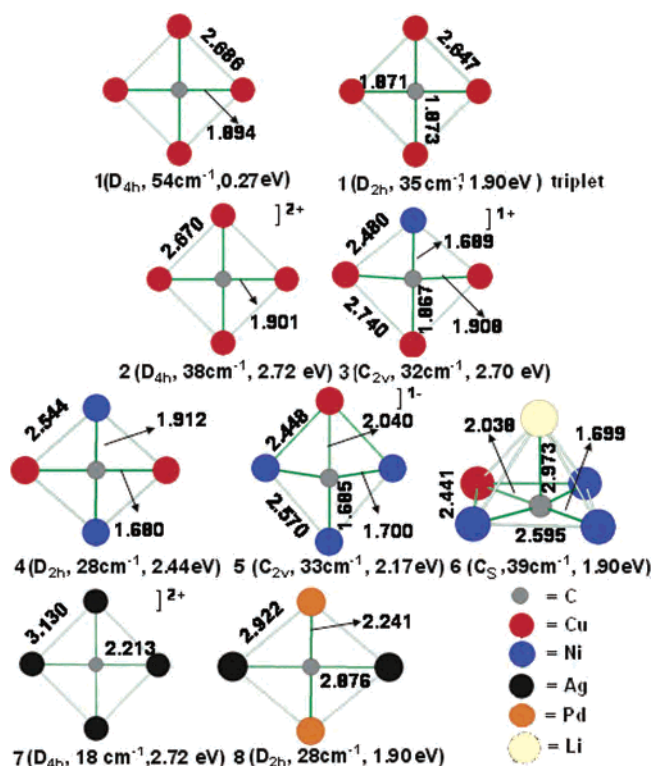


**Figure 1.** B3LYP/TZPP structures of the transition metal cages (for Ag, Pd, B3LYP/LANL2DZ ECP, and valence basis sets) containing planar tetracoordinate carbons. The selected bond lengths are in Å. The smallest vibrational frequency (mode corresponding to pyramidalization) and the HOMO–LUMO separations (in eV) are given for all the species.

optimized automatically, typically at low levels of theory to begin with. HF/STO-3G was chosen in the present application. Redundancies in each set (energies within 0.00001 au) are eliminated. The sets of kick runs are continued until no new structures are generated. Since no symmetry constraints are imposed, the geometries obtained should correspond to minima. The lowest-energy structures at the preliminary level (and others, which seem attractive) are then reoptimized and refined at the higher B3LYP/TZVPP level, followed by vibrational frequency computations.

### Structure and Energetics

The relatively short computed M–ptC bond lengths (in the 1.871–2.040 and 1.680–1.700 Å ranges for the species in Figure 1) indicate significant stabilization because these

(14) Musanke, U. E.; Jeitschko, W. *Z. Naturforsch. B* **1991**, *46*, 1177.  
 (15) Merschrod, E. F.; Tang, S. H.; Hoffmann, R. *Z. Naturforsch. B* **1998**, *53*, 322.  
 (16) Tsipis, C. A.; Karagiannis, E. E.; Kladou, P. F.; Tsipis, A. C. *J. Am. Chem. Soc.* **2004**, *126*, 12916.  
 (17) Li, S.-D.; Ren, G.-M.; Miao, C.-Q.; Jin, Z.-H. *Angew. Chem., Int. Ed.* **2004**, *43*, 1371. They reported ptC containing a  $D_{4h}$  hydronickel compound. However, the planar  $D_{4h}$  hydrocopper analogue ( $\text{Cu}_4\text{H}_4\text{C}$ ) was found to be a first-order saddle point, and pyramidal  $C_{4v}$  (in which the C atom lies about 0.5 Å above the  $\text{Cu}_4$  plane) was found to be the global minimum.  
 (18) Wannere, C. S.; Corminboeuf, C.; Wang, Z.-X.; Wodrich, M. D.; King, R. B.; Schleyer, P. v. R. *J. Am. Chem. Soc.* **2005**, *127*, 5701.  
 (19) Weigend, F.; Ahlrichs, R. *Phys. Chem. Chem. Phys.* **2005**, *18*, 3297.  
 (20) Hay, P. J.; Wadt, W. R. *J. Chem. Phys.* **1985**, *82*, 299.

(21) Frisch, M. J.; Trucks, G. W.; Schlegel, H. B.; Scuseria, G. E.; Robb, M. A.; Cheeseman, J. R.; Montgomery, J. A., Jr.; Vreven, T.; Kudin, K. N.; Burant, J. C.; Millam, J. M.; Iyengar, S. S.; Tomasi, J.; Barone, V.; Mennucci, B.; Cossi, M.; Scalmani, G.; Rega, N.; Petersson, G. A.; Nakatsuji, H.; Hada, M.; Ehara, M.; Toyota, K.; Fukuda, R.; Hasegawa, J.; Ishida, M.; Nakajima, T.; Honda, Y.; Kitao, O.; Nakai, H.; Klene, M.; Li, X.; Knox, J. E.; Hratchian, H. P.; Cross, J. B.; Bakken, V.; Adamo, C.; Jaramillo, J.; Gomperts, R.; Stratmann, R. E.; Yazyev, O.; Austin, A. J.; Cammi, R.; Pomelli, C.; Ochterski, J. W.; Ayala, P. Y.; Morokuma, K.; Voth, G. A.; Salvador, P.; Dannenberg, J. J.; Zakrzewski, V. G.; Dapprich, S.; Daniels, A. D.; Strain, M. C.; Farkas, O.; Malick, D. K.; Rabuck, A. D.; Raghavachari, K.; Foresman, J. B.; Ortiz, J. V.; Cui, Q.; Baboul, A. G.; Clifford, S.; Cioslowski, J.; Stefanov, B. B.; Liu, G.; Liashenko, A.; Piskorz, P.; Komaromi, I.; Martin, R. L.; Fox, D. J.; Keith, T.; Al-Laham, M. A.; Peng, C. Y.; Nanayakkara, A.; Challacombe, M.; Gill, P. M. W.; Johnson, B.; Chen, W.; Wong, M. W.; Gonzalez, C.; Pople, J. A. *Gaussian 03*, revision C.02; Gaussian, Inc.: Wallingford, CT, 2004.  
 (22) Saunders, M. J. *Comput. Chem.* **2004**, *25*, 621.  
 (23) Bera, P. P.; Sattelmeyer, K. W.; Saunders, M.; Schaefer, H. F.; Schleyer, P. v. R. *S. J. Phys. Chem. A* **2006**, *110*, 4287.

lengths are shorter than the sum of van der Waals radii (e.g., for Cu–C (2.190 Å) and Ni–C (2.150 Å)).<sup>24</sup> In addition, the rather short intramolecular metal–metal distances (<2.7 Å) favor cyclic electron delocalization and further stabilize the planar configurations relative to the corresponding tetrahedral forms.

Despite being a local minimum, **1** is not the most stable isomer as the butterfly ( $C_{2v}$ ) form is  $\sim 33.4$  kcal/mol more stable. In addition, the  $CCu_4$  subunits aggregate in the bulk.<sup>25</sup> The HOMO–LUMO energy separation of singlet **1** is small (0.27 eV), and the  $D_{2h}$  triplet electronic state is 22.9 kcal/mol lower in energy. Triplet **1** ( $D_{2h}$ ) is thus a better neutral candidate for the observation of a ptC (Figure 1). The removal of two electrons from  $CCu_4$  (**1**) generates the  $D_{4h}$   $CCu_4^{2+}$  dication (**2**); its HOMO–LUMO energy separation is substantial, 2.72 eV (Figure 1). Moreover, pyramidal ( $C_{4v}$ ) and butterfly ( $D_{2d}$ )  $CCu_4^{2+}$  starting geometries give the  $D_{4h}$  minima (**2**) upon optimization. The stability of **2** is further demonstrated by its large binding and atomization energy (24.5 and 28.9 eV, respectively, at the B3LYP/TZVPP level). The viability of **2** is consistent with the experimental characterization of the isoelectronic  $Cu_4Na^-$  cluster by Wang et al.<sup>26</sup> Although the neutral  $D_{4h}$   $Cu_4$  framework is electronically unstable by itself,<sup>27</sup> it is stabilized by the presence of a central atom and two additional electrons. This is especially so in **2**, since the vacant  $p_z$   $C^{2+}$  orbital interacts with the filled orbitals of the metal ring.

Remarkably, the isoelectronic analogues of  $Cu_4C^{2+}$ ,  $C_{2v}$   $CCu_3Ni^+$  (**3**),  $D_{2h}$   $CCu_2Ni_2$  (**4**), and  $C_{2v}$   $CCuNi_3^-$  (**5**), all are local minima and have ptC's. Like many anions, the  $CCuNi_3^-$  (**5**) HOMO has a positive eigenvalue (0.0007). However, the presence of the  $Li^+$  counterion in the monocapped  $CCuNi_3^-Li^+$  (**6**) precludes electron detachment; the HOMO energy is lowered to  $-0.1567$ . The  $C_s$  symmetry of **6** prevents perfect planarity of the  $CCuNi_3^-$  moiety, but the out-of-plane distortion is small. While  $D_{4h}$   $CNi_4^{2-}$ , our final member of the isoelectronic  $Cu \rightarrow Ni$  replacement series, also is a minimum, its HOMO–LUMO separation is large (1.9 eV). Interaction with the two  $Li^+$  counterions destroys the planarity of the  $CNi_4$  unit. Thus  $D_{4h}$   $CNi_4Li_2$  has one imaginary vibrational frequency associated with the out-of-plane motion of Ni leading to  $C_{4v}$  symmetry.

$CCu_4^{2+}$  (**2**) and  $CCu_3Ni^+$  (**3**) have the largest HOMO–LUMO separations and may be the best candidates for gas-phase experimental detection among the isoelectronic **2–6** set. Neutral  $D_{2h}$   $CCu_2Ni_2$  (**4**) is about 6 kcal mol<sup>-1</sup> more stable than its  $C_{2v}$  counterpart but is prone to aggregate.<sup>25</sup> Although  $D_{2h}$   $CAG_2Pd_2$  (**8**) is 7 kcal mol<sup>-1</sup> higher in energy than a  $C_1$  symmetry isomer (see Supporting Information),

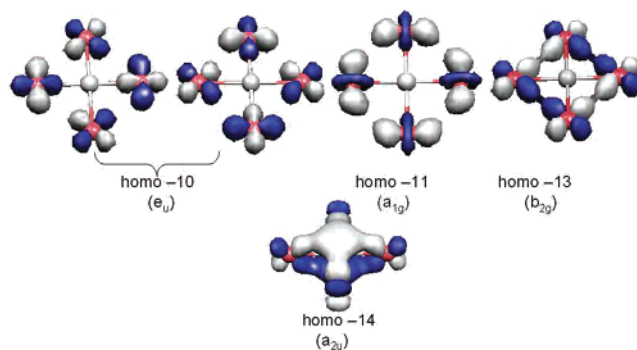


**Figure 2.** Illustrative molecular orbitals of  $CCu_4^{2+}$  ( $D_{4h}$ ) (B3LYP/TZVPP). The isosurface value is 0.05 au.

the isoelectronic  $D_{4h}$   $CAG_4^{2+}$  (**7**) may be viable. Attention also is called to the planar triplet state of neutral  $CCu_4$  (**1**).

### Molecular Orbital and NBO analysis

Molecular orbital (MO) analyses of **1–8** reveal features that stabilize the ptCs by interaction of the carbon  $p_z$  orbital with the transition metal ring skeleton. Note the important contribution of the perpendicular ptC p orbital to the delocalized  $\pi$   $a_{2u}$  HOMO–14 of  $CCu_4^{2+}$  depicted in Figure 2. (The full set of MO's is given in the Supporting Information.) The peripheral metal–metal bonding interactions of the other MO's shown in Figure 2 also favor the planar structures strongly.

Natural bond orbital (NBO) analyses<sup>28</sup> of **1–8** indicate considerable electron transfer from the surrounding metal atoms to the more electronegative carbons in the centers. For example, the atomic charges of the  $CCu_4^{2+}$  dication (**2**) are  $+0.89 e$  for Cu and  $-1.57 e$  for the ptC, while those for the neutral (**4**) are  $+0.38$  (Cu),  $+0.20$  (Ni) and  $-1.16 e$  (ptC). Such charge distributions show that the electron transfer is more effective from Cu than from Ni. NBO also reveals significant  $2p_z$  ptC orbital occupancies. Thus, the electronic population of the C atom valence shell is  $2s^{1.72}2p_x^{1.62}2p_y^{1.62}2p_z^{0.57}$  in **2**,  $2s^{1.62}2p_x^{1.47}2p_y^{1.48}2p_z^{0.78}$  in **3**,  $2s^{1.55}2p_x^{1.38}2p_y^{1.33}2p_z^{0.87}$  in **4**, and  $2s^{1.51}2p_x^{1.32}2p_y^{1.35}2p_z^{1.05}$  in **5**. The  $2p_z$  ptC orbital occupancies are in agreement with the Wang–Schleyer ptC bonding model (see above),<sup>10</sup> which is based conceptually on stabilization of a vacant  $2p_z$  ptC orbital through electron transfer. In addition, the ptC benefits from  $\sigma$  donation<sup>4</sup> by the electropositive transition metals justifying the relatively high occupancy of both the  $2p_x$  and  $2p_y$  carbon orbitals. Finally, the delocalized character of the in-plane C–M bonding is well illustrated by the atom–atom overlap weighted NAO bond orders, varying from 0.5 per C–Cu in  $CCu_4^{2+}$  to 0.7 for C–Ni in  $CCu_3Ni^+$  (see details in the Supporting Information).

### Magnetic Properties

$\delta^{13}C$  and the nucleus-independent chemical shift<sup>29</sup> (NICS) PW91/TZVPP all-electron DFT computations provide a more

(24) Lide, D. R.; Frederikse, H. P. R. *CRC Handbook of Chemistry and Physics*; CRC Press: New York, 1998; pp 9–51.

(25) The aggregation of two neutral  $CCu_4$  or  $CCu_2Ni_2$  subunits into their respective  $C_{2h}$  dimers is favored by more than 120 and 75 kcal mol<sup>-1</sup>, respectively (see Supporting Information).

(26) Lin, Y. C.; Sundholm, D.; Juselius, J.; Cui, L. F.; Li, X.; Zhai, H. J.; Wang, L. S. *J. Phys. Chem. A* **2006**, *110*, 4244.

(27) Neutral  $D_{4h}$   $Cu_4$  suffers from wave function instability problems at the DFT level (PW91PW91/LANL2DZ).

(28) Reed, A. E.; Curtiss, L. A.; Weinhold, F. *J. Chem. Rev.* **1988**, *88*, 899.

(29) (a) Schleyer, P. v. R.; Maerker, C.; Dransfeld, A.; Jiao, H.; Hommes, N. J. R. *E. J. Am. Chem. Soc.* **1996**, *118*, 6317. (b) Chen, Z.; Wannere, C. S.; Corminboeuf, C.; Puchta, R.; Schleyer, P. v. R. *Chem. Rev.* **2005**, *105*, 3842.



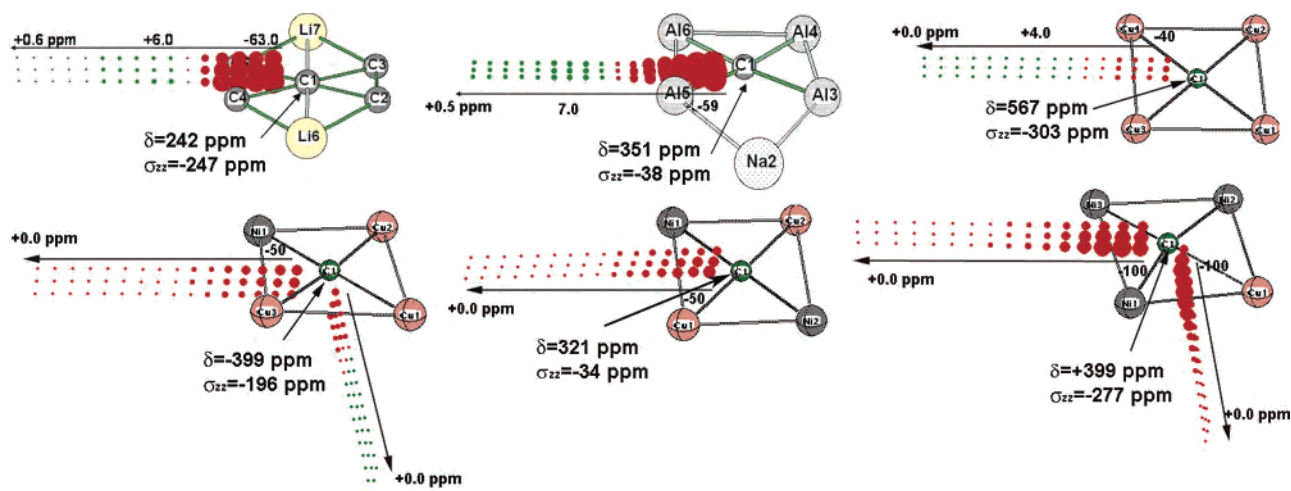


**Figure 3.** Two-dimensional grids ( $0.6 \times 5.0 \text{ \AA}$ ) of  $\text{NICS}_{zz}$  points and  $^{13}\text{C}$  chemical shifts ( $\delta$ ) for **2–5** (PW91/TZVPP)  $\text{Cu}_4\text{Na}^+$  (PW91/IGLOIII) and for the previously studied  $\text{C}_5\text{Li}_2$ .<sup>30</sup>

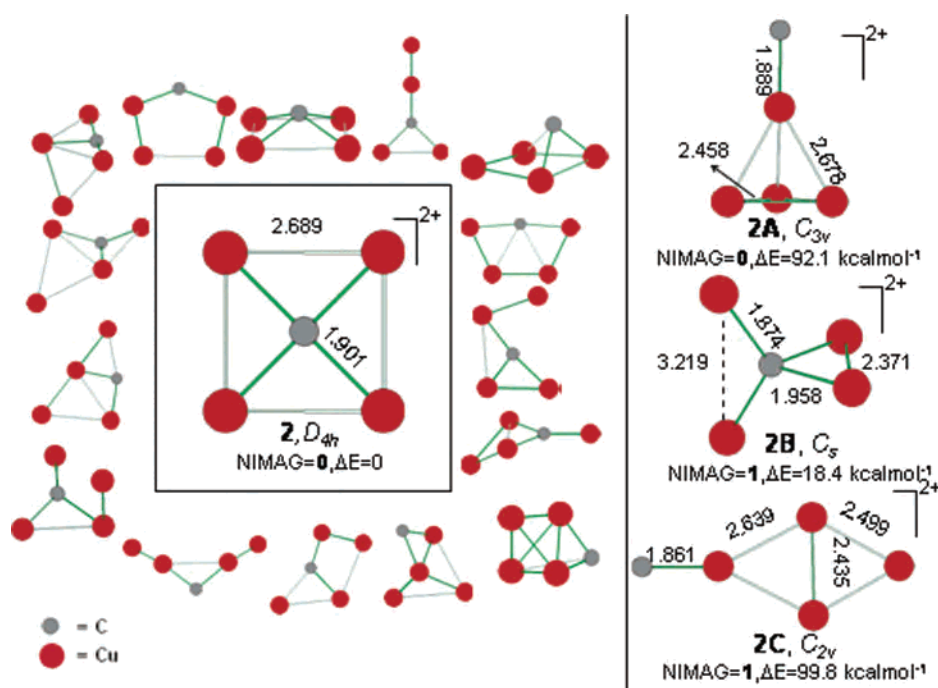


**Figure 4.** Three of the four stationary points of  $\text{CCu}_4^{2+}$  obtained at the B3LYP/TZVPP level are displayed on the right side. NIMAG is the number of imaginary harmonic frequencies.  $\Delta E$  is the energy relative to **2**. All distances are in angstroms. Illustrative preliminary structures, generated by the kick method at HF/STO-3G (see text) are shown on the left side. These all led to the ptC global minimum (**2**) upon further refinement at the higher theoretical level.

detailed understanding of the extent of cyclic electron delocalization in these systems. In particular, the  $\text{NICS}_{zz}$ <sup>29b,30</sup> index, which is closely related to the current density, reflects the magnetic response of a molecule toward a magnetic field applied perpendicularly to the plane (the  $z$  direction by the usual convention). Figure 3 displays grids of  $\text{NICS}_{zz}$  points and  $^{13}\text{C}$  chemical shifts for **2–5**,  $\text{Cu}_4\text{Na}^+$ , and the previously studied  $\text{C}_5\text{Li}_2$ ,<sup>31</sup> for comparison. The peculiar properties of the ptCs in **2–5** are best illustrated by their  $^{13}\text{C}$  NMR

chemical shifts (Figure 3), which differ dramatically from the usual  $\text{sp}^2$  carbon shielding range (120–220 ppm). The out-of-plane component of the carbon shielding tensor ( $\sigma_{zz}$ ) is more informative than the  $^{13}\text{C}$  chemical shift itself. Thus,  $\text{C}_5\text{Li}_2$  and  $\text{CCu}_4^{2+}$  (**2**) have a fairly large  $^{13}\text{C}-\sigma_{zz}$  value ( $>300$  ppm) as compared to that of **3–5** ( $<200$  ppm). This greater magnitude is consistent both with a larger decrease of electron density at the planar tetracoordinated carbon and with a stronger electronic delocalization in the bare copper and carbon rings.

The magnetic behavior of  $\text{C}_5\text{Li}_2$  is known<sup>31</sup> to be similar to benzene: both have large diatropic (magnetic aromaticity)

(30) (a) Fowler, P. W.; Steiner, E. *Mol. Phys.* **2000**, *98*, 945. (b) Steiner, E.; Fowler, P. W.; Jennesskens, L. W. *Angew. Chem., Int. Ed.* **2001**, *40*, 362. (c) Corminboeuf, C.; Heine, T.; Seifert, G.; Schleyer, P. v. R. *Phys. Chem. Chem. Phys.* **2004**, *6*, 273. (d) Fallah-Bagher-Shaidaei, H.; Wannere, C. S.; Corminboeuf, C.; Puchta, R.; Schleyer, P. v. R. *Org. Lett.* **2006**, *8*, 863.

(31) Merino, G.; Mendez-Rojas, M. A.; Beltran, I. H.; Corminboeuf, C.; Heine, T.; Vela, A. *J. Am. Chem. Soc.* **2004**, *126*, 16160.

regions inside and deshielding regions outside the ring.  $\text{CCu}_4^{2+}$  (**2**) is confirmed to be a promising candidate for isolation as it exhibits the same  $\text{NICS}_{zz}$  pattern as  $\text{C}_5\text{Li}_2$  (Figure 3) and benzene: its deshielding outside is weaker (up to +3.5 ppm vs 5.6 ppm for  $\text{C}_5\text{Li}_2$ ). In sharp contrast, **4** and **5** do not exhibit a deshielding region but remain weakly diatropic outside the ring: it vanishes at  $\sim 5$  Å. Such unexpected magnetic behavior is inconsistent with Pople's ring-current model<sup>32</sup> and hence with the existence of a diatropic ring current around the metal framework of **4** and **5**. Interestingly, the magnetic behavior of **3** is similar to that of **4** and **5** but with a fairly weak increase of the deshielding ( $> 2.5$  ppm) along the direction perpendicular to a Cu–Cu bond.

### Exploration of the Potential Energy Surface

Finally, to explore the potential energy surface of our most promising candidate,  $\text{CCu}_4^{2+}$  (**2**), a total of 1000 kick jobs in independent sets of 50 were performed at the HF/STO-3G level of theory. The procedure is explained in the Computational Details section, above. The best structures from the initial level were refined at B3LYP/TZVPP. Only two minima, the global minimum, **2**, and the 92.1 kcal/mol less-stable local minimum, **2A** (Figure 4), were located on the PES of  $\text{CCu}_4^{2+}$ . Most of the "candidates" generated at the lower HF/STO-3G level did not survive and optimized to **2** at B3LYP/TZVPP. We have also located two transition structures, both of which are involved (as shown by their IRCs) in different degenerate permutations of Cu atoms: **2C** is the transition state between two stereomutated **2As**, and **2B** is the transition state between two stereomutated **2's** (Figure 4).

(32) Pople, J. A. *J. Chem. Phys.* **1956**, *24*, 1111.

All kick optimizations proceed in point group  $C_1$ , but often lead very nearly to higher symmetries, which may then be imposed prior to the further refinement. Additional MP2/TZVPP calculations (details in Supporting Information) confirm that the dication **2** is a minimum and much more stable than the alternative geometries.

We have also explored the potential energy surfaces for  $\text{CCu}_2\text{Ni}_2$ ,  $\text{CCu}_3\text{Ni}^+$ , and  $\text{CCuNi}_3^-$  extensively using the kick method.<sup>22,23</sup> The structures with  $\text{ptC}'$ 's also were found to be the global minima. (Geometries and energies for the isomers are given in the Supporting Information.)

As illustrated by the  $\text{CM}_4$  systems (M are the combinations of Cu, Ni, Ag, and Pd) analyzed here, bare four-membered transition metal rings are good candidates for stabilizing planar tetracoordinate carbons. While neutral examples are likely to aggregate, their isoelectronic cationic analogues and  $\text{CCu}_4^{2+}$  in particular are good prospects for detection by gas-phase photoelectron spectroscopy,<sup>33,34</sup> when compared to highly accurate electron binding energy.

**Acknowledgment.** This work was financially supported by NSF Grant CHE-0209857 and partly by the Petroleum Research Fund (Grant 41888-AC4).

**Supporting Information Available:** Cartesian coordinates for the stationary points, atom–atom overlap weighted NAO bond order for Cu and Cu–Ni clusters, full set of MOs for  $\text{CCu}_4^{2+}$ , and alternative structures for  $\text{CCu}_2\text{Ni}_2$ ,  $\text{CCu}_3\text{Ni}^+$ , and  $\text{CCuNi}_3^-$  obtained by the kick method. This material is available free of charge via the Internet at <http://pubs.acs.org>.

IC060802G

(33) Wang, L. S.; Cheng, H. S.; Fan, J. *J. Chem. Phys.* **1995**, *102*, 9480.

(34) Wang, L. S.; Wu, H. In *Advances in Metal and Semiconductor Clusters IV. Cluster Materials*; Duncan, M. A., Ed.; JAI: Greenwich, U.K., 1998; pp 299–343.